European Review for Medical and Pharmacological Sciences 2018; 22: 6551-6559

Protective effect of cyclosporine on inflammatory injury of renal tubular epithelial cells

Y.-Q. ZHANG, Y. CHEN, Y.-M. DING, T.-H. YU

Department of Nephrology, The Affiliated Jiangyin Hospital of Southeast University Medical College, Wuxi, China

Abstract. – OBJECTIVE: This study aims to explore the protective effect of cyclosporine on inflammation-induced renal tubular epithelial cells and its potential mechanism.

MATERIALS AND METHODS: Human kidney-2 (HK-2) cells were induced by transforming growth factor-β (TGF-β) for constructing an inflammatory injury model. Cells were then treated with different concentrations of cyclosporine for further investigating the biological functions. Cell viability was detected via cell counting kit-8 assay (CCK-8). The cytotoxicity was detected via lactate dehydrogenase (LDH) release assay. Expression levels of cell damage factors and mammalian target of rapamycin (mTOR) pathway-related genes were detected via polymerase chain reaction (PCR), immunofluorescence and Western blotting, respectively.

RESULTS: TGF-β inhibited the viability of HK-2 cells, increased expressions of tumor necrosis factor-α (TNF-α), interleukin-1β (IL-1β) and apoptosis-related genes. Cyclosporine treatment greatly reversed the cell damage on HK-2 cells induced by TGF-β. Expression levels of mTOR pathway-related genes were downregulated after cyclosporine treatment.

CONCLUSIONS: Cyclosporine protects HK-2 cells from inflammatory injury via regulating mTOR pathway.

Key Words:
Cyclosporine, HK-2 cells, TGF-β, mTOR.

Introduction

Chronic kidney injury (CKI) is a result of many pathological factors, including diabetes, hypertension, infection, atherosclerosis, renal artery or ureteral obstruction, etc.[1]. Injuries of glomerular, renal tubular or renal vascular will cause pathological changes in renal structure and function. With the pathological progress of CKI, it eventually develops into fibrosis, decreased nephrons and scar formation[2]. One of the main symptoms of CKI is proteinuria, which is caused by a large number of microvascular damages due to vascular endothelial dysfunction[3]. Researches have suggested that cyclosporine exerts a therapeutic effect on CKI *via* endothelium repair and vascular endothelial growth factor (VEGF) downregulation. VEGF is a key cytokine leading to endothelial cell morphological changes and proteinuria development regulation[4].

Water-soluble ingredients are the main active ingredients of cyclosporine (CSA) in the treatment of CKI. Clinical studies have shown that the mixture of a variety of salvianolic acid, total cyclosporine phenolic acid, can reduce plasma level of endothelin-1 and urinary protein, thereafter improving renal function in CKI patients[5]. Total cyclosporine phenolic acid can improve the renal function of CKI rats through inhibiting the epithelial to mesenchymal transition (EMT) of glomerular basement membrane *via* downregulating endothelin. Moreover, it can delay the renal interstitial fibrosis of rats undergoing unilateral ureteral occlusion (UUO) by inhibiting the formation of transforming growth factor-β1 (TGF-β1). Total cyclosporine phenolic acid can significantly reduce the expressions of α-smooth muscle actin (α-SMA), vimentin, TGF-β1, matrix metalloproteinase-2 in renal tissues of UUO rats. It can also improve the renal interstitial fibrosis and renal function[6]. In *in vitro* studies, salvianolic acid B inhibits the TGF-β1-induced EMT in human kidney-2 (HK-2) cells and antagonizes the TGF-β1-induced fibronectin (FN) upregulation via inhibiting the Jagged/Notch signaling pathway[7].

Mammalian target of rapamycin (mTOR) is a kind of highly-conserved phosphoinositide 3-kinase (PI3K)-related kinase. It is a key regulator of cell growth and proliferation, which can be regulated by growth factor, nutrition, energy and other signals. It also plays a role through PI3K/

Corresponding Author: Yaoquan Zhang, MD; e-mail: 13626238242@163.com

serine/threonine kinase (AKT) or Ras/Extracellular regulated protein kinases (ERK) signaling pathways. Inactivation of the mTOR-signaling pathway results in cell cycle arrest in G1 phase and triggers apoptosis. Relative studies pointed out that mTOR is involved in the renal dysfunction and fibrosis in CKI via activating macrophage activity and inflammatory factors[8]. In addition, mTOR can cause chronic renal tubular injury through binding to receptors on the tubular epithelial cells[9]. It is concluded that mTOR pathway plays a role in the kidney damage, fibrosis and renal tubular epithelial damage, etc.

This study focuses on the protective effect of CSA on inflammatory injury of renal tubular epithelial cells and its underlying mechanism.

Materials and Methods

Cells and Experimental Reagents

HK-2 cells were commonly selected for the *in vitro* study of CKI[10,11]. HK-2 cells were purchased from Shanghai Institute of Cell Research, Chinese Academy of Sciences (Shanghai, China). Dulbecco's modified eagle medium (DMEM) and fetal bovine serum (FBS) were purchased from Sigma-Aldrich (St. Louis, MO, USA). Tumor necrosis factor-α (TNF-α) and interleukin-1β (IL-1β) detection kits were purchased from Roche (Basel, Switzerland). Experimental antibodies were obtained from Santa Cruz Biotechnology, Inc. (Santa Cruz, CA, USA). Other reagents were purified in analytical grade.

Cell Culture and Modeling

HK-2 cells were cultured in DMEM containing 10% FBS in an incubator containing 5% CO_2 at 37°C. In the preliminary experiment, cells were treated with different concentrations of TGF-β for 24 h, 48 h and 72 h, respectively. We found that 5 ng/mL TGF-β induction for 72 h exhibited the strongest inhibitory effect on HK-2 cells (data not shown). Serum-free culture was replaced, and cells were induced with transforming growth factor-β (TGF-β) (5 ng/mL) for 24 h, followed by CSA treatment for 3 d. Culture medium was replaced every day.

Cell Counting Kit-8 (CCK-8) Assay

Cells in the logarithmic growth phase were centrifuged after digestion with 0.25% trypsin. The supernatant was discarded and cells were resuspended in Dulbecco's Modified Eagle Medium (DMEM) containing 10% FBS. Cell density was adjusted to 1.0×10^5 cells/mL. Cell suspension was inoculated into the 96-well plate (100 μL per well) and cultured in an incubator containing 5% CO_2 at 37°C for 4 h. After intervention according to the experimental grouping (4 wells/group), 10 μL of CCK-8 solution (Dojindo, Kumamoto, Japan) were added into each well and cells were maintained in an incubator containing 5% CO_2 at 37°C for 4 h. The absorbance at 450 nm was determined using the microplate reader.

Lactate Dehydrogenase (LDH) Detection

Cells in the logarithmic growth phase were digested with 0.25% trypsin and EDTA (Ethylene Diamine Tetraacetic Acid) (Thermo Fisher Scientific, Waltham, MA, USA). Cells were resuspended in DMEM containing 10% FBS and inoculated into the 96-well plate at a density of 5.0×10^3 cells/mL, with three replicates in each group. After cell adherence and drug intervention, the culture plate was maintained in an incubator containing 5% CO_2 at 37°C for 24 h. The supernatant was taken (20 μL each well) and the corresponding LDH reagents were added according to the kit instructions. After the solution was placed at room temperature for 3 min, 1 cm optical cuvette was used for zero set with 440 nm double distilled water. OD (optical density) value of each tube was determined using the microplate reader. For unit definition, 1000 mL culture solution were reacted with substrate for 15 min at 37°C, and 1 gmol pyruvic acid was produced in the reaction system as l unit. The LDH content in the medium was calculated according to the formula.

Enzyme-Linked Immunosorbent Assay (ELISA)

Cell culture medium was collected into 3 k concentrated centrifuge tube, followed by centrifugation at 7500 rpm/min for 20 min. The operation liquid was prepared according to the instructions and 100 μL assay diluent were added into each well of the 96-well plate for two groups, with 6 well per group. The first group was the standard curve group, and the prepared working solution was added into 6 wells. The second group was added with the conditioned medium. The culture medium collected from each group was added from the first well, incubated at 37°C for 2 h, and washed with 400 μL wash buffer for 3 times. All the liquid was removed finally. 200 μL conjugate were added into each well for incubation at 37°C for 2 h and washed with 400

μL wash buffer for 3 times. Subsequently, 200 μL substrate were added and incubated at 37°C for half an hour in dark. Finally, 50 μL terminator were added into each well, and the 96-well plate was slightly shaken and mixed. The OD value was measured at a wavelength of 450 nm. The standard curve was drawn, and the HGF concentration in each sample was obtained *via* solving equations.

Terminal Deoxynucleotidyl Transferase dUTP Nick-end Labeling (TUNEL) Assay

Apoptosis of HK-2 cells was detected following the instructions of ApopTag Plus Peroxidase *In Situ* Apoptosis Detection Kit (Chemicon, Millipore, Billerica, MA). Each kidney sample was sliced for 5 sections and stained with TUNEL solution, followed by re-stain of methyl green. The amount of TUNEL-positive cells in 10 randomly selected fields was calculated under a high power microscope (200×).

Flow Cytometry Analysis of the Cell Apoptosis

HK-2 cells in logarithmic growth period were seeded in the 6-well plate and treated with corresponding intervention for 24 h. After cells were washed with phosphate-buffered saline (PBS) twice, they were resuspended in the binding solution and incubated at room temperature for 15 min in dark. Subsequently, cells were incubated with 5 μL AnnexinV-FITC and 5 μL propidium iodide (PI) in dark, followed by flow cytometry detection.

Immunofluorescence

After cell confluence was up to 95-100% on coverslips, the cells were fixed with 4% formaldehyde, permeabilized with 0.5% Triton X-100 at 37°C for 20 min and sealed with FBS. Subsequently, cells were incubated TGF-β (1:100), 4EBP1 (1:100) and mTOR (1:100) at 4°C overnight. After incubation with corresponding secondary antibody, the cells were re-stained with DAPI (4',6-diamidino-2-phenylindole) (Sigma-Aldrich, St. Louis, MO, USA) and mounted with 95% glycerol. Observations and imaging were conducted under a confocal fluorescence microscope.

RNA Extraction and Quantitative Reverse Transcription-Polymerase Chain Reaction (qRT-PCR)

Cells were digested and transferred to the 1.5 mL ribozyme-free Eppendorf tube (EP). 1 mL TRIzol was added (Invitrogen, Carlsbad, CA, USA), followed by blowing and beating evenly until cells were sufficiently denatured. After trichloromethane was added, the mixture was vigorously stirred and placed on ice for 15 min, followed by centrifugation at 12000 rpm/min at 4°C for 15 min. 500 mL isopropyl alcohol were added, mixed and placed on ice for 15 min. Centrifugation was performed at 12000 rpm/min, 4°C for 15 min. Next, the supernatant was discarded and 75% ethanol was added to wash the precipitate, followed by centrifugation at 8000 rpm/min, 4°C for 5 min. The supernatant was discarded, and the precipitate was dried and dissolved in 20 μL diethyl pyrocarbonate (DEPC) water (Beyotime, Shanghai, China) for concentration measurement. The reverse transcription system was added for the reverse transcription reaction according to the sample concentration. After the reaction system of complementary Deoxyribose Nucleic Acid (cDNA) was synthesized, PCR amplification was performed. Primer design software Primer premier 5.0 (Palo Alto, CA, USA) was used for primer sequence design: Bax, F: 5'-CAGAAAACATTTCAGCCGCCACTC-3', R: 5'-CCTTTTGCTTCAGGGTTTCATCCAG-3'; Bcl-2, F: 5'-CTGAGTACCTGAACCGGCATCT-3', R: 5'-GAGACAGCCAGGAGAAGTCAAAC-3'; 4EBP1, F: 5'-AGCCGTAGGACGCAATGAT-3', R: 5'-ACAGAGGCACAAGGAGGTATGT-3'; β-actin, F: 5'-GGCCAGAAAGACTGCTATGTG-3', R: 5'-GCTCGTTGTAGAAAGTGTGGTG-3'. The real-time fluorescence signal was collected after each cycle, and the amplification and dissolution curves were recorded.

Western Blotting

Cells in each group were collected and the total protein was extracted using the protein extraction kit. The protein concentration was determined using bicinchoninic acid (BCA) method (Pierce, Rockford, IL, USA). After protein quantification, 5 μL 5×loading buffer were added and the protein was boiled at 99°C for 5 min. Protein sample was separated *via* sodium dodecyl sulfate polyacrylamide gel electrophoresis (SDS-PAGE). The concentration of concentrated gel was 5%, while that of lower separation gel was 10%. Voltage in the constant voltage separation were set as 90 V for upper gel for 90 min, and 150 V for separation gel for 150 min. The protein was separated until the bromophenol blue reached the bottom of the gel. The gel, filter paper and polyvinylidene difluoride

(PVDF) membrane (Millipore, Billerica, MA, USA) were placed sequentially in the electrophoresis tank for membrane transfer. After that, the membrane was removed, labeled and sealed in 5% skim milk powder at 37°C for 1 h. After the sealing fluid was washed clean with PBS for three times, membranes were incubated overnight with primary antibody (diluted at 1:850) at 4°C in dark. On the next day, the primary antibody was recycled, and the membrane was washed with PBS for 3 times (5 min/time). The secondary antibody horseradish-peroxidase (HRP)-labeled goat anti-rabbit IgG, diluted at 1:5000) was added for incubation on the shaking table at 37°C for 2 h. The secondary antibody was discarded, and the membrane was washed with PBS for 3 times (15 min/time). Finally, the image gray was scanned using ImageJ after color development in the developing instrument.

Statistical Analysis

Data were presented as mean ± standard deviation. One-way analysis of variance (ANOVA) was used for intergroup comparison, followed by Least Significant Difference as its Post-Hoc Test. $p < 0.05$ indicated the difference was statistically significant. Statistical Product and Service Solutions (SPSS) 17.0 software (SPSS Inc., Chicago, IL, USA) was used for data analysis.

Results

Cyclosporine Alleviated Decreased Cell Viability Induced by TGF-β

Cell viability in blank group, TGF-β group, TGF-β + different concentrations of cyclosporine (0.1 μM, 1 μM, 2 μM, 4 μM and 8 μM) group was measured *via* CCK-8 assay. The results showed that the cell viability in TGF-β group was significantly decreased compared with that in control group ($p < 0.05$). There were no significant differences between 0.1 μM group, 1 μM group and TGF-β group. The cell viability in 2 μM group and 4 μM group was significantly higher than that in TGF-β group ($p < 0.05$). However, the cell viability in 8 μM group was slightly decreased compared with that in TGF-β group (Figure 1A).

Cyclosporine Alleviated the Cell Damage Induced by TGF-β

Cell damage was detected *via* LDH assay. The results showed that the LDH release in TGF-β group was significantly increased compared with that in control group ($p < 0.05$). There were no significant differences between 0.1 μM group, 1 μM group and TGF-β group. LDH releases in 2 μM group and 4 μM group were significantly lower than that in TGF-β group ($p < 0.05$). However, LDH release in 8 μM group was slightly increased compared with that in TGF-β group (Figure 1B).

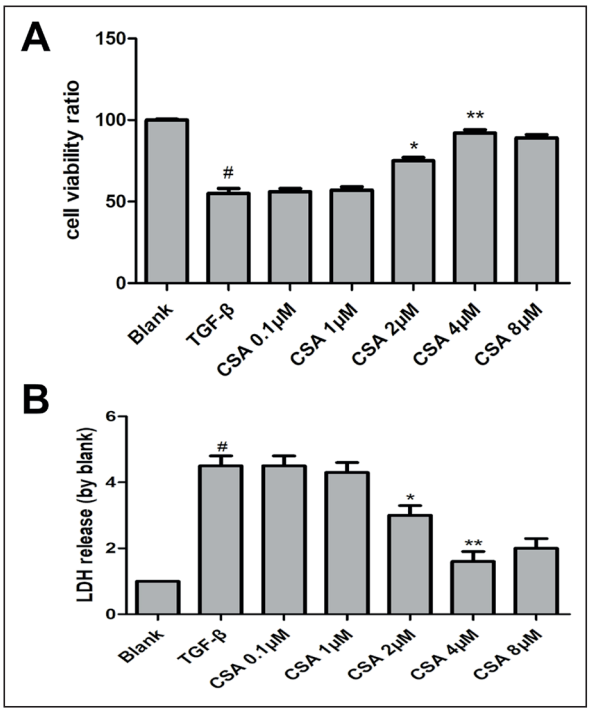

Figure 1. Drug concentration detection test. ***A,*** Detection of cell viability *via* CCK-8 assay. The cell viability of blank group, TGF-β group, TGF-β + different concentrations of cyclosporine group (0.1 μM, 1 μM, 2 μM, 4 μM and 8 μM) was detected *via* CCK-8 assay. ***B,*** Detection of cytotoxicity *via* LDH assay. Cytotoxicity in TGF-β group and TGF-β + different concentrations of cyclosporine group (0.1 μM, 1 μM, 2 μM, 4 μM and 8 μM) was detected *via* the ratio of LDH release to that in blank group. #Compared with blank group, $p < 0.05$; *Compared with TGF-β group, $p < 0.05$; **Compared with 2 μM group, $p < 0.05$.

Cyclosporine Reduced the Release of Inflammatory Factors Induced by TGF-β

The releases of TNF-α and IL-1β in supernatant of blank group, TGF-β group and TGF-β + cyclosporine (4 μM) group were detected *via* immunofluorescence and ELISA, respectively. We found that the release of TNF-α in TGF-β group was 2-fold higher than that in blank group ($p < 0.05$). However, the release of TNF-α was significantly decreased after cyclosporine treatment ($p < 0.05$). Similar results were obtained

in detecting IL-1β release (Figure 2). The results proved that cyclosporine can significantly reduce the release of inflammatory factors induced by TGF-β.

Cyclosporine Reduced the Production of Apoptotic Proteins Induced by TGF-β

TUNEL assay and flow cytometry indicated that apoptotic cells in TGF-β group were much more than those of blank group. However, TGF-β + cyclosporine group showed less apoptosis compared with that in TGF-β group ($p < 0.05$, Figure 3A and 3B).

The mRNA expressions of mTOR pathway downstream molecules were detected *via* PCR. The results showed that the mRNA expression of Bax in TGF-β group was significantly higher than that in blank group ($p < 0.05$), whereas it was significantly decreased after cyclosporine treatment ($p < 0.05$, Figure 3C). The mRNA expression of Bcl-2 in TGF-β group was significantly lower than that in blank group ($p < 0.05$), whereas it was significantly increased after cyclosporine treatment ($p < 0.05$, Figure 3C). The expressions of apoptosis-related proteins, Bax, Bcl-2, caspase3 and cleaved-caspase3, were detected *via* Western blotting. The results showed that the ratio of cleaved-caspase3/caspase3 in TGF-β group was significantly higher than that in blank group ($p < 0.05$), whereas it was significantly decreased after cyclosporine treatment ($p < 0.05$, Figure 3D-3J). The results proved that cyclosporine can significantly reduce the TGF-β-induced apoptosis.

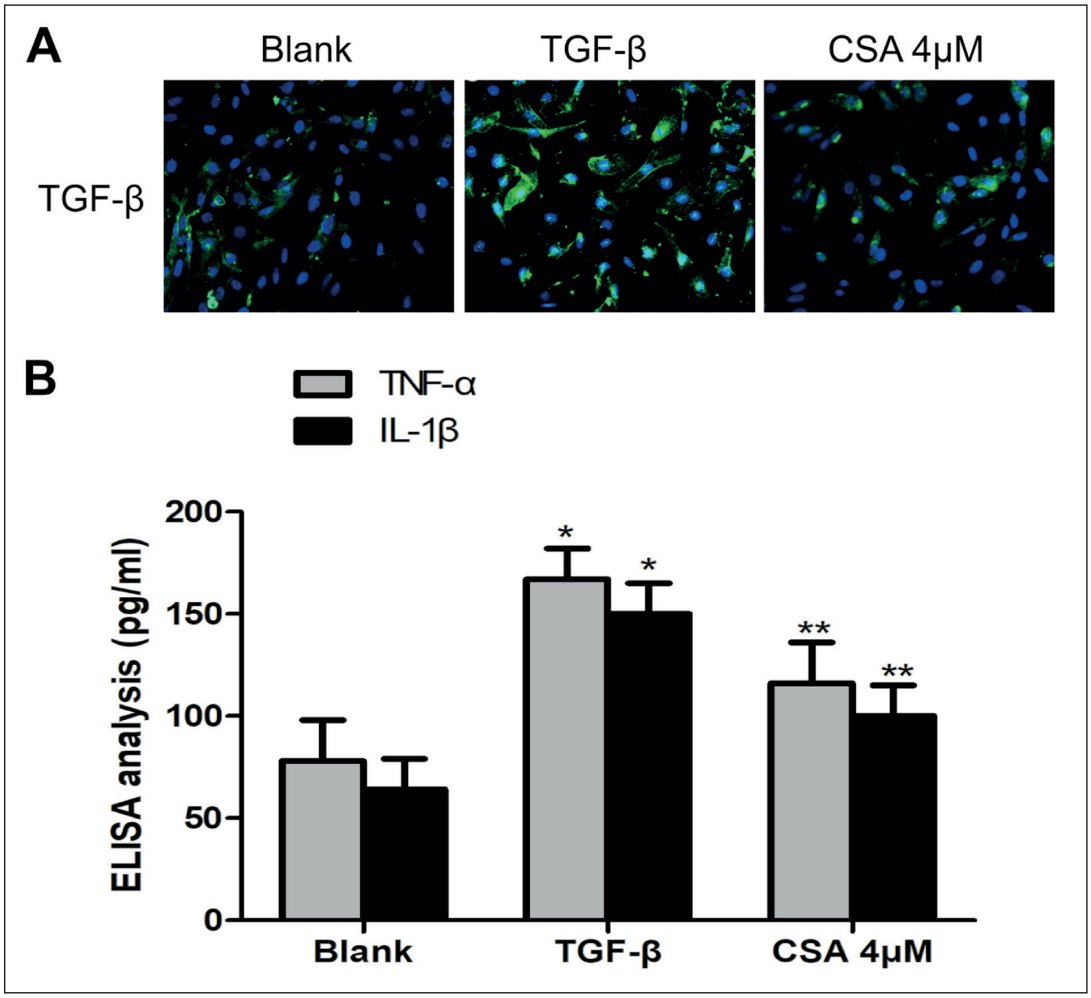

Figure 2. Detection of inflammatory factor release *via* immunofluorescence and ELISA. ***A,*** The release of TNF-α in supernatant of blank group, TGF-β group and TGF-β + cyclosporine (4 μM) group was detected by immunofluorescence. ***B,*** The releases of TNF-α and IL-1β in supernatant of blank group, TGF-β group and TGF-β + cyclosporine (4 μM) group were detected *via* ELISA. *Compared with blank group, $p < 0.05$; **Compared with TGF-β group, $p < 0.05$.

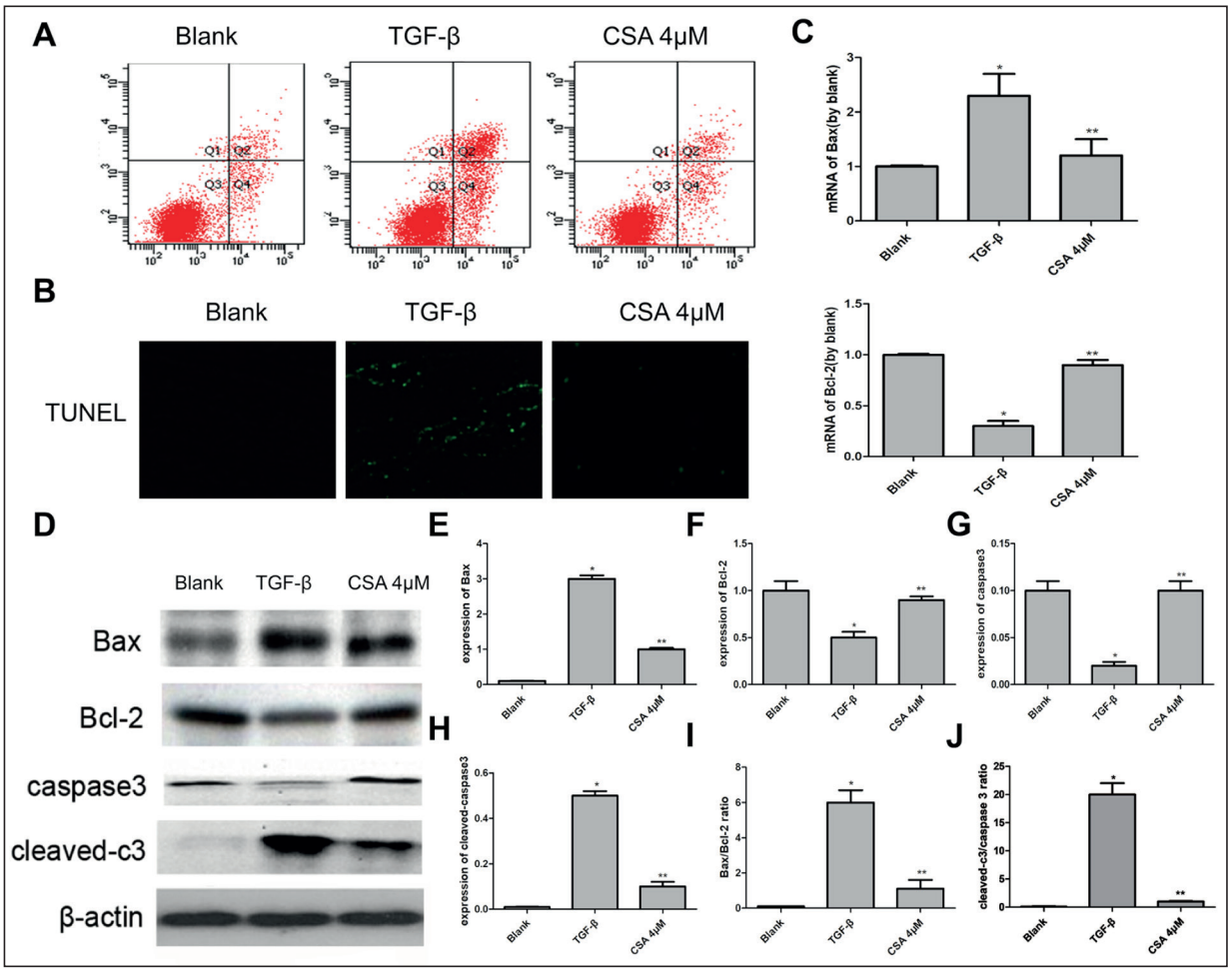

Figure 3. Detection of expressions of apoptosis related pathway. ***A,*** The efficiencies of cell apoptosis in blank group, TGF-βgroup and TGF-β+ cyclosporine (4 μM) group were detected via flow cytometry. ***B,*** Representative images (200×) of TUNEL immunostaining in kidney tissues. Quantification of TUNEL-positive cells by average number of 5 HPF in different groups. ***C,*** The mRNA expressions of apoptosis-related molecules, Bcl-2 and Bax, in blank group, TGF-β group and TGF-β + cyclosporine (4 μM) group were detected *via* PCR. ***D,*** The expressions of apoptosis-related molecules, Bcl-2 and Bax, cleaved-caspase3 and caspase3 in blank group, TGF-β group and TGF-β + cyclosporine (4 μM) group were detected *via* Western blotting. ***E-H,*** Data statistics of gray scan of apoptosis-related molecules, Bcl-2 and Bax, cleaved-caspase3 and caspase3 in blank group, TGF-β group and TGF-β + cyclosporine (4 μM) group. ***I-J,*** Data statistics of ratios of apoptosis-related molecules, Bcl-2 and Bax, cleaved-caspase3 and caspase3 in blank group, TGF-β group and TGF-β + cyclosporine (4 μM) group. *Compared with blank group, $p < 0.05$; **Compared with TGF-β group, $p < 0.05$.

Cyclosporine Inhibited the Activation of mTOR Pathway Induced by TGF-β

Immunofluorescence indicated that the fluorescence densities of 4EBP1 and mTOR in TGF-β group were higher compared with those in blank group, which were remarkably decreased in TGF-β + cyclosporine group ($p < 0.05$, Figure 4A and 4B).

Whether the protective effect of cyclosporine on cell function of HK-2 cells was related to mTOR pathway was further studied. The mRNA expressions of mTOR pathway downstream molecules were detected *via* PCR. The results showed that the mRNA expression of eukaryotic translation initiation factor 4E-binding protein (4EBP1) in TGF-β group was significantly higher than that in blank group ($p < 0.05$), but it was significantly decreased after cyclosporine treatment ($p < 0.05$, Figure 4C). Protein expressions of mTOR, phosphorylated mTOR (p-mTOR) and 4EBP1 were detected *via* Western blotting. The results showed that the ratio of p-mTOR/mTOR and the expression of 4EBP1 in TGF-β group were significantly higher than those in blank group ($p < 0.05$), but it was significantly decreased after cyclosporine

treatment ($p < 0.05$, Figure 4D-4J). The results proved that cyclosporine can remarkably inhibit the activity of mTOR pathway induced by TGF-β.

Discussion

Cyclosporine and its aqueous solution are widely applied in the prevention and treatment of CKI. Since cyclosporine ketone in traditional water decoction is very difficult to be dissolved, the water-soluble component is considered as the main material basis[6]. Cyclosporine structure is the chemical parent nucleus of a variety of salvianolic acids, and other components of cyclosporine in the body are hydrolyzed into cyclosporine. In this study, *in vitro* CKI model was established by TGF-β induction in renal tubular epithelial HK-2 cells. HK-2 cells were then treated with different concentrations of cyclosporine. The results showed that cyclosporine could protect HK-2 cells from CKI in a concentration-dependent manner. Through the detection of cell viability and LDH release, we found that 2 μM cyclosporine had protective effect on HK-2 cells, which reached the peak at 4 μM. Therefore, 4 μM cyclosporine was selected for follow-up study.

Inflammation plays an important role in the occurrence and progression of CKI[12]. In the CKI animal model, the expressions of nuclear factor-κB (NF-κB), IL, monocyte chemoattractant protein-1 (MCP-1) and other pro-inflammatory

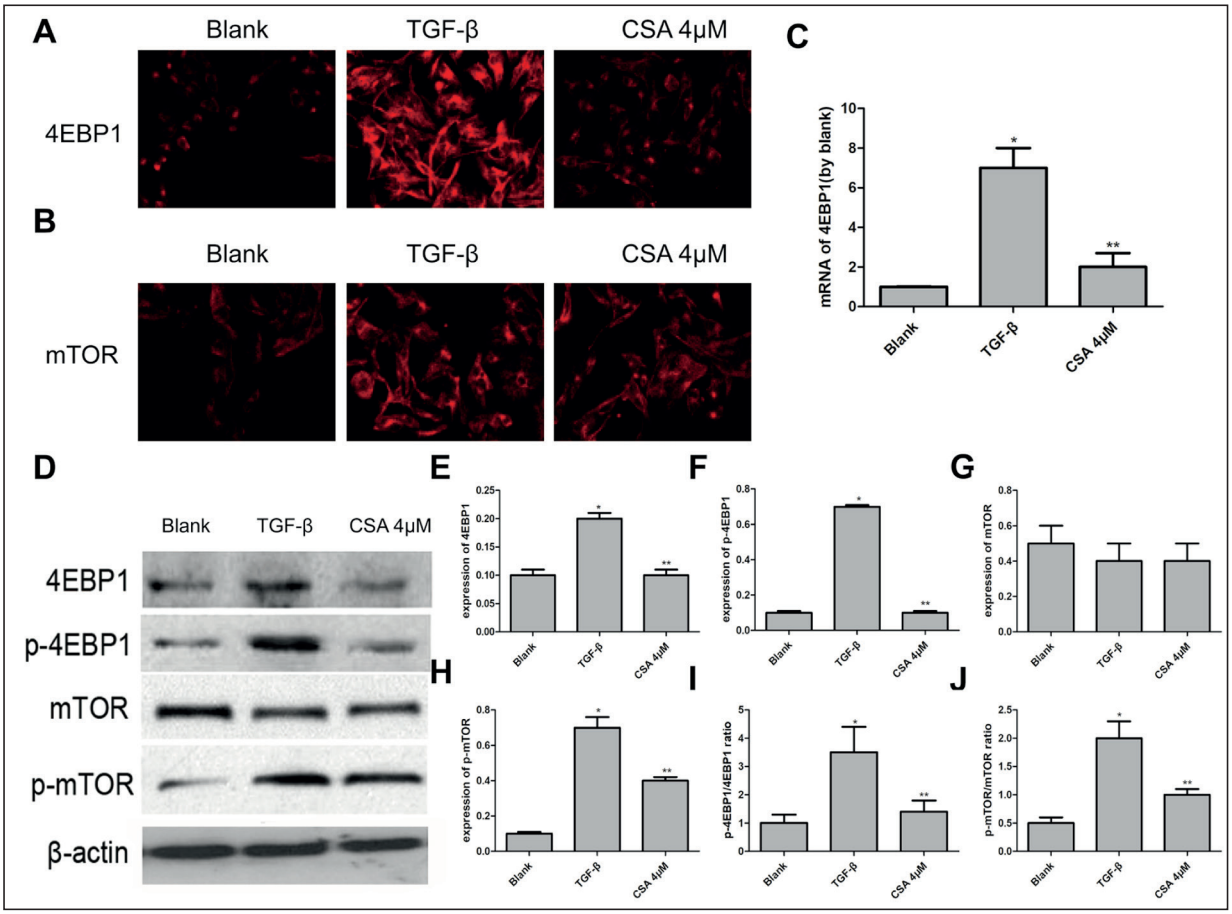

Figure 4. Detection of expressions of mTOR-related pathway. ***A-B,*** The expressions of two EMT markers (4EBP1 and mTOR) in HK-2 cells were assayed using a Nikon (Melvile, NY, USA) Eclipse TE300 fluorescence microscope (magnification 200×). ***C,*** The mRNA expression of 4EBP1 in blank group, TGF-β group and TGF-β + cyclosporine (4 μM) group was detected *via* PCR. ***D,*** The expressions of cellular pathways-related molecule, 4EBP1, mTOR and p-mTOR in blank group, TGF-β group and TGF-β + cyclosporine (4 μM) group were detected *via* Western blotting. ***E-H,*** Data statistics of gray scan of cellular pathways-related molecule, 4EBP1, mTOR and p-mTOR in blank group, TGF-β group and TGF-β + cyclosporine (4 μM) group. ***I-J,*** Data statistics of ratios of cellular pathways-related molecule, 4EBP1, mTOR and p-mTOR in blank group, TGF-β group and TGF-β + cyclosporine (4 μM) group. *Compared with blank group, $p < 0.05$; **Compared with TGF-β group, $p < 0.05$.

cytokines are significantly up-regulated[13]. It has been reported that TGF-β recruits inflammatory cells to the injury site via upregulating SMAD3-mediated MCP-1 expression, thereby regulating the renal inflammatory response[14,15]. In this study, it was found that 4 μM cyclosporine could significantly reduce the releases of TNF-α and IL-1β induced by TGF-β. In addition to inflammatory response, recent studies[16] have suggested that the excessive apoptosis of renal tubular epithelial cells would lead to the atrophy of renal tubules and deterioration of renal function. In this study, it was found that cyclosporine could significantly reduce the ratio of Bax/Bcl-2 and cleaved-caspase3/caspase3, indicating that cyclosporine could remarkably alleviate TGF-β-induced apoptosis.

At present, works[8] have shown that mTOR pathway is closely related to the inflammatory response, and renal fibrosis progression in CKI. The specific role of mTOR pathway in renal function is controversial. Some studies [17,18] have found that mTOR pathway exerts a protective role in cell transformation and renal function improvement. However, most studies on CKI showed that the mTOR pathway activates the renal injury. In addition, corresponding receptors of mTOR play important roles during the renal fibrosis progression caused by TGF-β/SMAD3 pathway[18]. In order to further investigate the mechanism in the protective effect of cyclosporine on HK-2 cells, the expressions of mTOR-related pathway proteins were detected. The results showed that cyclosporine could significantly reduce the expressions of p-mTOR and p70, suggesting that the protective role of cyclosporine in HK-2 cells may be related to mTOR pathway. In the present study, we only explored partial downstream genes in mTOR pathway. Further investigations need to be carried out to explore the in-depth mechanism of mTOR pathway in CKI.

Conclusions

We found that cyclosporine downregulated the expressions of the apoptosis-related proteins through the inhibition of mTOR pathway, thereby protecting renal tubular epithelial HK-2 cells from CKI caused by TGF-β.

Conflict of Interest

The Authors declare that they have no conflict of interests.

References

1) Lopez-Hernandez FJ, Lopez-Novoa JM. Role of TGF-beta in chronic kidney disease: an integration of tubular, glomerular and vascular effects. Cell Tissue Res 2012; 347: 141-154.
2) Eddy AA. Molecular basis of renal fibrosis. Pediatr Nephrol 2000; 15: 290-301.
3) Zhang W, Li X, Zhou SG. Ablation of carbohydrate-responsive element-binding protein improves kidney injury in streptozotocin-induced diabetic mice. Eur Rev Med Pharmacol Sci 2017; 21: 42-47.
4) Chao CY, Lii CK, Ye SY, Li CC, Lu CY, Lin AH, Liu KL, Chen HW. Docosahexaenoic acid inhibits vascular endothelial growth factor (VEGF)-induced cell migration via the GPR120/PP2A/ERK1/2/eNOS signaling pathway in human umbilical vein endothelial cells. J Agric Food Chem 2014; 62: 4152-4158.
5) Jiang C, Zhu W, Yan X, Shao Q, Xu B, Zhang M, Gong R. Rescue therapy with tanshinone IIA hinders transition of acute kidney injury to chronic kidney disease via targeting GSK3beta. Sci Rep 2016; 6: 36698.
6) Cariddi LN, Escobar FM, Sabini MC, Campra NA, Bagnis G, Decote-Ricardo D, Freire-de-Lima CG, Manas F, Sabini LI, Dalcero AM. Phenolic acid protects of renal damage induced by ochratoxin a in a 28-days-oral treatment in rats. Environ Toxicol Pharmacol 2016; 43: 105-111.
7) Murea M, Park JK, Sharma S, Kato H, Gruenwald A, Niranjan T, Si H, Thomas DB, Pullman JM, Melamed ML, Susztak K. Expression of notch pathway proteins correlates with albuminuria, glomerulosclerosis, and renal function. Kidney Int 2010; 78: 514-522.
8) Chen H, Zhu J, Liu Y, Dong Z, Liu H, Liu Y, Zhou X, Liu F, Chen G. Lipopolysaccharide induces chronic kidney injury and fibrosis through activation of mTOR signaling in macrophages. Am J Nephrol 2015; 42: 305-317.
9) Yin W, Naini SM, Chen G, Hentschel DM, Humphreys BD, Bonventre JV. Mammalian target of rapamycin mediates kidney injury molecule 1-dependent tubule injury in a surrogate model. J Am Soc Nephrol 2016; 27: 1943-1957.
10) Oshiro S, Ishima Y, Maeda H, Honda N, Bi J, Kinoshita R, Ikeda M, Iwao Y, Imafuku T, Nishida K, Miyamura S, Watanabe H, Otagiri M, Maruyama T. Dual therapeutic effects of an albumin-based nitric oxide donor on 2 experimental models of chronic kidney disease. J Pharm Sci 2018; 107: 848-855.
11) Liu H, Xiong J, He T, Xiao T, Li Y, Yu Y, Huang Y, Xu X, Huang Y, Zhang J, Zhang B, Zhao J. High uric acid-induced epithelial-mesenchymal transition of renal tubular epithelial cells via the TLR4/NF-kB signaling pathway. Am J Nephrol 2017; 46: 333-342.

12) Chen S, Zhou S, Wu B, Zhao Y, Liu X, Liang Y, Shao X, Holthofer H, Zou H. Association between metabolically unhealthy overweight/obesity and chronic kidney disease: the role of inflammation. Diabetes Metab 2014; 40: 423-430.

13) Vaziri ND, Liu SM, Lau WL, Khazaeli M, Nazertehrani S, Farzaneh SH, Kieffer DA, Adams SH, Martin RJ. High amylose resistant starch diet ameliorates oxidative stress, inflammation, and progression of chronic kidney disease. PLoS One 2014; 9: e114881.

14) Meng XM, Chung AC, Lan HY. Role of the TGF-beta/BMP-7/Smad pathways in renal diseases. Clin Sci (Lond) 2013; 124: 243-254.

15) Rodriguez-Barbero A, Dorado F, Velasco S, Pandiella A, Banas B, Lopez-Novoa JM. TGF-beta1 induces COX-2 expression and PGE2 synthesis through MAPK and PI3K pathways in human mesangial cells. Kidney Int 2006; 70: 901-909.

16) Ohse T, Inagi R, Tanaka T, Ota T, Miyata T, Kojima I, Ingelfinger JR, Ogawa S, Fujita T, Nangaku M. Albumin induces endoplasmic reticulum stress and apoptosis in renal proximal tubular cells. Kidney Int 2006; 70: 1447-1455.

17) Chen G, Dong Z, Liu H, Liu Y, Duan S, Liu Y, Liu F, Chen H. mTOR signaling regulates protective activity of transferred CD4+Foxp3+ T cells in repair of acute kidney injury. J Immunol 2016; 197: 3917-3926.

18) Li J, Ren J, Liu X, Jiang L, He W, Yuan W, Yang J, Dai C. Rictor/mTORC2 signaling mediates TGFbeta1-induced fibroblast activation and kidney fibrosis. Kidney Int 2015; 88: 515-527.